

Accurate non-relativistic photoionization cross section for He at non-resonant photon energies

This article has been downloaded from IOPscience. Please scroll down to see the full text article.

2011 J. Phys. B: At. Mol. Opt. Phys. 44 035004

(<http://iopscience.iop.org/0953-4075/44/3/035004>)

View [the table of contents for this issue](#), or go to the [journal homepage](#) for more

Download details:

IP Address: 141.89.199.236

The article was downloaded on 28/03/2012 at 18:30

Please note that [terms and conditions apply](#).

Accurate non-relativistic photoionization cross section for He at non-resonant photon energies

Alexander Stark¹ and Alejandro Saenz^{1,2}

¹ AG Moderne Optik, Institut für Physik, Humboldt-Universität zu Berlin, Newtonstr. 15, D-12489 Berlin, Germany

² Kavli Institute for Theoretical Physics, University of California, Santa Barbara, CA 93106-4030, USA

E-mail: alejandro.saenz@physik.hu-berlin.de

Received 24 August 2010, in final form 26 November 2010

Published 19 January 2011

Online at stacks.iop.org/JPhysB/44/035004

Abstract

The total single-photon ionization cross section was calculated for helium atoms in their ground state. Using a full configuration-interaction approach the photoionization cross section was extracted from the complex-scaled resolvent. Our results agree with an earlier *B*-spline-based calculation in which the continuum is box discretized within a relative deviation of less than 0.06% in the energy range from 28 to 59 eV. On the other hand, above the He⁺⁺ threshold our results agree very well to a recent Floquet calculation. Thus, our calculation confirms the previously reported deviations from the experimental reference data outside the claimed error estimate. In order to extend the calculated spectrum to very high energies, an analytical hydrogenic-type model tail is introduced that should become asymptotically exact for infinite photon energies. Its universality is investigated considering also H⁻, Li⁺ and HeH⁺. With the aid of the tail corrections to the dipole approximation are estimated.

(Some figures in this article are in colour only in the electronic version)

1. Introduction

Since the beginning of quantum mechanics the photoionization cross section (PCS) of the helium atom was investigated in a number of experiments and numerical calculations. Helium is one of the simplest quantum mechanical systems that is relatively easily experimentally accessible, but also amenable to very accurate calculations. At the same time, it is theoretically challenging, since even within non-relativistic quantum mechanics the helium atom cannot be solved analytically. Due to these special characteristics the helium PCS is very attractive for a direct comparison of theory and experiment.

In 1994, high-precision measurements of the PCS were performed by Samson *et al* [1, 2] using a double-ion chamber and a high-voltage spark discharge. Since then the therein reported values for the PCS of helium with an estimated accuracy of 1–1.5% in the low-energy range and about 2% for the high-energy part beyond the double-ionization threshold were used in many applications in, e.g., astrophysics,

plasma physics and chemistry. Recently, the PCS of helium also became relevant for the characterization of novel light sources such as high-harmonic radiation or free-electron lasers (FEL). The supposedly very accurately known PCS of helium provides a natural way for tests and calibrations (especially of the intensity) of these new-generation light sources [3, 4]. For example, in the SASE (self-amplified stimulated emission) experiment at FLASH (Hamburg) the two-photon double photoionization of helium is used to determine the duration of ultrashort femtosecond pulses [5]. Thereby, the nonlinear autocorrelation of direct $\text{He} \rightarrow \text{He}^{2+} + 2\text{e}^-$ and sequential $\text{He} \rightarrow \text{He}^+ + \text{e}^- \rightarrow \text{He}^{2+} + 2\text{e}^-$ double-ionization processes is measured. The first step of the sequential process corresponds, of course, to single-photon ionization of He.

However, despite the development of new theoretical approaches and the access to increasing computational power it has so far not been possible to reproduce the experimental reference data in [1, 2] to the therein claimed accuracy. Supposedly very accurate theoretical values for the PCS of helium from the ionization threshold to photon energies of

71 eV were reported by Venuti *et al* in [6]. This was a follow-up work to the one presented in [7] which extended to 2 keV but was less accurate. The calculations were performed within the configuration-interaction (CI) approach in which the orbitals were expressed in B splines (for the radial part) multiplied by spherical harmonics (for the angular part). The finite range of the adopted B splines leads to a box-type discretization for the continuum wavefunctions. From convergence studies and the agreement between the results obtained using the length, velocity or acceleration form of the dipole operator the authors of [6] estimated the error to be smaller than 0.001 Mb which corresponds to a relative error of 0.014–0.063%. In comparison to the experimental data in [1, 2] a deviation of up to about 2.6% was, however, found in the considered low-energy range which is almost twice the estimated experimental error.

More recently, Ivanov and Kheifets implemented a Floquet approach and calculated the PCS of helium starting at a photon energy of 80 eV using Hylleraas-type basis functions [8]. Again, the authors claim to reach an accuracy of the order of the fraction of a per cent, but find noticeable deviations from the experimental reference data that easily reach up to 6%. On the other hand, for a single value of the photon energy, 40 eV, good agreement was found with the theoretical results in [6]. As a consequence, the non-relativistic dipole and infinite-mass approximations used in both calculations appear to be inadequate or either the calculations or the experimental data are less accurate than claimed by the respective authors. In order to shed more light on this question, we performed calculations with a different theoretical approach in which the orbitals used in the subsequent CI method are constructed from Slater functions. Furthermore, the PCS is extracted from the complex-scaled resolvent and thus no box discretization as, e.g., in [6] is used. We extend our *ab initio* results to very high photon energies by introducing an analytical, hydrogen-like model tail. This is of interest, for example, in view of the present efforts of extending the FEL sources to the x-ray regime, as with the LCLS (linac coherent light source) at Stanford, the XFEL (x-ray free electron laser) in Hamburg or the SPring8-XFEL project in Japan. The universality of the here introduced tail is investigated by also considering the other two-electron systems H^- , Li^+ , and even the molecular ion HeH^+ . The tail is finally used to obtain an analytical estimate of the first-order correction to the dipole approximation.

2. Method and computational details

2.1. *Ab initio* calculation

In view of the large mass difference of the He nucleus and the electrons we adopt the infinite-mass approximation for the He nucleus in our calculations. This should be justified, since for the PCS of the He^+ ion, for which the analytical result is known, the size of the modification due to the finite mass of the nucleus is only of the order of 0.1%. It is expected that this effect has a similar size in the case of the neutral He atom. Furthermore, there should not be a strong energy-dependent contribution due to the finite mass. In fact, for the ion it is energy independent.

Relativistic effects should also be negligible, because their scaling parameter, the nuclear charge, is evidently a small value in the case of helium atoms. Furthermore, in this work we consider only the non-resonant part of the PCS. Relativistic effects are expected to manifest themselves especially for the resonances associated with autoionizing continuum states. In a recent work [14] a multi-configuration Dirac–Fock method was used to determine the values 0.99 and 0.01 for the Fano parameter ρ^2 of the singlet 1P_1 state and the triplet 3P_1 state, respectively. Based on this result we may conclude that relativistic effects at non-resonant energies are expected to be definitely smaller than 1%.

To obtain the wavefunctions and the corresponding energy eigenvalues of He we used a direct expansion in Slater-type orbitals (STOs). In the calculation of the 1S helium ground state the same basis-set parameters were used as in our recent calculation of the final-state spectrum of helium atoms after β decay of tritium anions [9]. The previous results for a large number of energy eigenvalues exhibited very good agreement with the literature values. For the 1P states we modified the 1S basis set as to adapt it to the different symmetry. As a result, we used 360 STOs leading to 3331 configuration state functions (CSFs) for all 1P states and 555 STOs resulting in 3481 CSFs for the 1S ground state. The number of CSFs is essentially limited by the fact that the STO basis set is not orthogonal, i.e. over complete. To reach a high level of accuracy we constructed our basis set with the highest number of CSFs but avoided linear-dependency problems at the same time. More details about the structure of the basis set and the construction of the symmetry-adapted CSFs used in the subsequent CI calculation can be found in [9].

The PCS σ is related to the optical oscillator strength density df/dE by the relation [10]

$$\sigma = \frac{\pi e^2 \hbar}{2\epsilon_0 m_e c} \frac{df(E)}{dE} = 109.7609 \text{ Mb} \frac{df(E)}{dE} \text{ eV} \quad (1)$$

with the electron mass m_e and charge e , the reduced Planck constant \hbar , the electric constant ϵ_0 and the speed of light in vacuum c . Using atomic units ($m_e = 1$, $e = 1$, $\hbar = 1$) the df/dE can be evaluated from the dipole transition probabilities $P(E)$

$$\left(\frac{df(E)}{dE} \right)_{\text{au}} = 2 \begin{cases} EP(E) & \text{in length form} \\ P(E)/E & \text{in velocity form.} \end{cases} \quad (2)$$

Finally the $P(E)$ can be extracted from the complex-scaled resolvent according to [11, 12]

$$P(E) = \frac{1}{\pi} \text{Im} \left\{ \sum_k \frac{\langle \Psi_i^S(\theta^*) | \hat{d}(\theta) | \Psi_k^P(\theta) \rangle \langle \Psi_k^P(\theta^*) | \hat{d}(\theta) | \Psi_i^S(\theta) \rangle}{E_k^P(\theta) - E_i^S(\theta) - E} \right\}. \quad (3)$$

The complex-scaling angle is denoted by θ and $\langle \Psi(\theta^*) |$ is the biorthonormal eigenstate to $|\Psi(\theta)\rangle$. It is obtained from the latter by a transposition and complex conjugation of the angular part, while the radial part is only transposed but not

conjugated. A variation of the angle θ allows the determination of an optimal angle θ_{opt} by requiring

$$\left. \frac{\partial P(E)}{\partial \theta} \right|_{\theta_{\text{opt}}} = \min. \quad (4)$$

In other words, the best approximation of $P(E)$ is obtained with that value of θ for which $P(E)$ shows the smallest dependence on θ . For more details about complex scaling see [9, 11, 13] and references therein. An application of this method for the photoionization of the molecular ion HeH^+ was described in [12].

In equation (3) the $|\Psi_k^{\text{P}}\rangle$ are the final helium ^1P wavefunctions and E_k^{P} are the associated energy eigenvalues. Analogous definitions apply to the ^1S initial state. The operator \hat{d} describes the coupling of an atomic electron to a (classical) electromagnetic field. Thereby the latter is represented by a plane wave in the spatial domain, $e^{i\mathbf{k}\cdot\mathbf{r}}$, with the wave vector \mathbf{k} and the spatial vector \mathbf{r} . Without loss of generality we can assume the wave is propagating along the z axis and the operator becomes in length and velocity forms

$$\hat{d}_l = -e^{ik\hat{z}}\hat{z} \quad (5)$$

and

$$\hat{d}_v = -e^{ik\hat{z}}\hat{v}_z, \quad (6)$$

respectively. For sufficiently low energies the dipole approximation $e^{ik\hat{z}} \approx 1$ can be applied to a high level of reliability. The complex-scaled versions of the operators are simply given by $\hat{d}_l(\theta) = -e^{+i\theta}\hat{z}$ and $\hat{d}_v(\theta) = -e^{-i\theta}\hat{v}_z$. For an N -electron system the electronic part of the operator is simply the sum of the N one-electron operators.

2.2. Analytical model for high photon energies

For very high photon energies we introduce an analytic tail. The concept behind its construction is that in the case of single-photon ionization the ejected electron takes away a large fraction of the energy of the absorbed photon. Thus it escapes very fast from the nucleus and the remaining (spectator) electron. Therefore, the fast electron experiences the remaining system (with a maximum screening of the nucleus by the spectator electron) to a good approximation as a point charge Z_f which is the sum of the charges of all remaining particles. (In the case of a He atom, the escaping electron experiences the remaining He^+ ion as a point charge with $Z_f = +1$.) As a result, we may approximate the final two-electron wavefunction as (the spin part is omitted for better readability)

$$|\tilde{\Psi}^{1s\mathcal{E}l}(\mathcal{E})\rangle = 2^{-\frac{1}{2}}[|1s^{Z_i}\mathcal{E}l^{Z_f}\rangle + |\mathcal{E}l^{Z_f}1s^{Z_i}\rangle] \quad (7)$$

with the hydrogen-like ground-state wavefunction with effective charge Z_i :

$$|1s^{Z_i}\rangle = \frac{Z_i^{3/2}}{\sqrt{\pi}} e^{-rZ_i}, \quad (8)$$

and the energy-normalized Coulomb continuum l -wavefunction for electron energy \mathcal{E} and charge Z_f :

$$|\mathcal{E}l^{Z_f}\rangle = \frac{2\sqrt{Z_f}(2r\kappa)^l}{(2l+1)!\sqrt{1-e^{-\frac{2\pi Z_f}{\kappa}}}} \prod_{s=1}^l \sqrt{s^2 + \frac{Z_f^2}{\kappa^2}} e^{-ir\kappa} \times {}_1F_1\left(\frac{iZ_f}{\kappa} + l + 1, 2l + 2, 2ir\kappa\right) Y_l^m(\theta, \phi), \quad (9)$$

with $\kappa = \sqrt{2\mathcal{E}}$. ${}_1F_1$ is the confluent hypergeometric function of the first kind and Y_l^m represents a spherical harmonic. The initial ^1S state is approximated as a product of two hydrogenic s orbitals with the same effective charge Z_i :

$$|\tilde{\Psi}^{1s^2}\rangle = |1s^{Z_i}1s^{Z_i}\rangle. \quad (10)$$

Of course this simple mean-field approach does not take into account the correlation in the motion of the two electrons but, as will be shown below, this disadvantage can be partly compensated by adjusting the effective charge Z_i .

In the model it is assumed that during the (fast) photoionization process (escape of the emitted electron) the spectator electron has no time to relax. As a consequence, the effective charge Z_i of the spectator electron remains the same in the initial (10) and the final (7) wavefunctions, but changes from Z_i to Z_f for the fast escaping electron.

Using this model we derive an analytical formula for the PCS for two-electron systems at high photon energies. When using the length-form representation of the dipole operator it reads in atomic units

$$\begin{aligned} \tilde{\sigma}_0^L(E) &= N \frac{512 \exp\left(-\frac{4Z_f \arctan(\kappa/Z_i)}{\kappa}\right) E Z_i^3 Z_f (Z_f - 2Z_i)^2 (Z_f^2 + \kappa^2)}{3(1 - \exp\left(-\frac{2\pi Z_f}{\kappa}\right))(Z_i^2 + \kappa^2)^6} \end{aligned} \quad (11)$$

with $\kappa = \sqrt{2\mathcal{E}} = \sqrt{2(E-I)}$, the photon energy E , the ionization potential I and the number of electrons N . The integral that occurs in the derivation of equation (11) can be solved using the corresponding maths described in [17]. Since our two-electron model adopts approximate wavefunctions the corresponding commutator relation leading to equivalence between length and velocity forms of the dipole operator is not fulfilled. For the velocity form of the dipole operator the model cross section becomes

$$\begin{aligned} \tilde{\sigma}_0^V(E) &= N \frac{128 \exp\left(-\frac{4Z_f \arctan(\kappa/Z_i)}{\kappa}\right) Z_i^5 Z_f (Z_f^2 + \kappa^2)}{3(1 - \exp\left(-\frac{2\pi Z_f}{\kappa}\right))E(Z_i^2 + \kappa^2)^4} \\ &= \left(\frac{Z_v(Z_v^2 + \kappa^2)}{2E(Z_f - 2Z_v)}\right)^2 \tilde{\sigma}_0^L(E). \end{aligned} \quad (12)$$

To distinguish the effective initial-state charges of the different representations we have introduced a new parameter Z_v that is the velocity-form analogue of Z_i introduced above for the length form. The results of both representations are compared and discussed in section 3.2.

It should be noted that for the one-electron case with $N = 1$ and $Z_i = Z_v = Z_f = \sqrt{2I}$ equations (11) and (12) are also evidently applicable for H-like systems. In this case

one obtains the same result with both equations. It agrees to the one given in [17] and proposed as an approximate tail also for the generalized oscillator strength density in [15]. The main feature of the model tail derived in this work is the distinction of the effective charges in the initial state (Z_i or Z_v) and the final state (Z_f). This additional degree of freedom improves the accuracy of the model for two-electron systems like He. Clearly, as discussed below for the example of HeH^+ , the present tail can also be adopted for molecular systems. In the spirit of the Born–Oppenheimer approximation it may be useful to adopt in such a case an internuclear-separation-dependent electron binding energy $I(R)$ instead of the experimental ionization potential [18–20].

Through its simplicity the tail model offers the possibility of studying analytically effects beyond the dipole approximation. Since the model becomes better for higher energy it is valid in the regime where the wavelength of the electric field may approach or even extend below the magnitude of 1 nm and is thus comparable to inner-atomic distances. To estimate these effects in helium we derived expressions for the first-order corrections to the dipole approximation. In this case the one-electron interaction operator in length form is given by

$$\hat{d}_l = -\hat{z} \exp(ik\hat{z}) \approx -\hat{z} - iE\alpha\hat{z}^2 \quad (13)$$

with the photon energy $E = \hbar k = (k/\alpha)$ (in au) and the fine-structure constant α . Since the initial state given in equation (10) has ^1S symmetry, the correction term $iE\alpha\hat{z}^2$ couples it only to final states with either ^1S or ^1D symmetry. In the spirit of the model one then has to substitute $|\mathcal{E}p^{Z_f}\rangle$ in equation (7) with $|\mathcal{E}s^{Z_f}\rangle$ and $|\mathcal{E}d^{Z_f}\rangle$ for the continuum states with ^1S and ^1D symmetry, respectively.

Since two distinct final states are reached at a given energy, the (incoherent) superposition of the cross sections into the ^1S and ^1D channels is given by

$$\tilde{\sigma}_1^L(E) = \tilde{\sigma}_0^L(E) (1 + (E\alpha)^2 (A_s^2 + A_d^2)) \quad (14)$$

with

$$A_s = \frac{6Z_i(\kappa^2 - 2Z_f^2 - Z_i(Z_i - 3Z_f)) + 2Z_f(Z_f^2 - 2\kappa^2)}{\sqrt{3}(Z_f - 2Z_i)\sqrt{Z_f^2 + \kappa^2}(Z_i^2 + \kappa^2)} \quad (15)$$

and

$$A_d = \frac{4(Z_f - 3Z_i)\sqrt{Z_f^2 + 4\kappa^2}}{\sqrt{15}(Z_f - 2Z_i)(Z_i^2 + \kappa^2)}. \quad (16)$$

In the case of the ^1S final states one obtains formally a term $\langle \mathcal{E}s^{Z_f} | 1s^{Z_i} \rangle \langle 1s^{Z_i} | \hat{z}^2 | 1s^{Z_i} \rangle$ which can be interpreted as a shake up of the electrons. It is an artefact from the unequal treatment of the two electrons in our model. Since in this case only one bound electron interacts with the electromagnetic field, the other electron (which will be ejected) plays the role of the spectator and consequently experiences no relaxation. Thus to stay consistent within our model we have to exchange the effective charges in this term to $\langle \mathcal{E}s^{Z_i} | 1s^{Z_i} \rangle \langle 1s^{Z_f} | \hat{z}^2 | 1s^{Z_i} \rangle$ which due to orthogonality of the $|\mathcal{E}s^{Z_i}\rangle$ and $|1s^{Z_i}\rangle$ orbitals vanishes.

We successfully tested the derived expressions for the cross sections in the one-electron case $Z = Z_i = Z_f$ with the aid of the sum rule [21]

$$S_0(k) = \sum_n 2(E_n - E_0) |\langle 0 | \hat{z}^k | n \rangle|^2 = k^2 \langle 0 | \hat{z}^{2k-2} | 0 \rangle \quad (17)$$

in which \sum includes a summation over bound states and an integration over the continuum of states. Furthermore, $|0\rangle$ denotes the initial state, e.g. the ground state.

In the case $k = 1$ (dipole approximation) the sum-rule result is equal to the number of electrons, $S(1) = 1$, and for $k = 2$ (corrections) one finds $S(2) = 4/Z^2$. By applying the model to the He^+ ion ($Z = 2$) we obtain $S_0(1) = 0.999\,999\,80$ and $S_0(2) = 0.999\,999\,73$, if bound-state transition probabilities of the He^+ wavefunctions up to the 2000th state were summed up and the optical oscillator strength density of the continuum states was integrated numerically.

Alternatively to the described tail, an asymptotic representation of the cross section is often used as an estimate in the high-energy regime. The asymptotic limit of our length-form model tail is (in atomic units)

$$\tilde{\sigma}_0^L(E) \approx N \frac{8\sqrt{2}Z_i^3(Z_f - 2Z_i)^2}{3\pi} E^{-7/2}. \quad (18)$$

It should be noted, however, that the analytic tail in (11) possesses a much larger validity regime than the asymptotic expression in (18), since it shows good agreement with experiment and *ab initio* theory already for much lower photon energies.

As mentioned above the length and velocity representations of the dipole operator lead to different expressions for the model tail. However, one may use the different representations to perform a consistency check of our model and to learn about the best values for the parameters Z_i or Z_v . For energies near infinity where the model is surely applicable the representations should lead to equivalent values. Thus we demanded the identity of the length and velocity model tails in the first order of the asymptotic expansion. The asymptotic limit of the model tail in velocity representation is

$$\tilde{\sigma}_0^V(E) \approx N \frac{8\sqrt{2}Z_v^5}{3\pi} E^{-7/2}. \quad (19)$$

Combining (18) and (19) allows the determination of a relation between Z_i and Z_v and to define a new parameter Z_v^* that fulfils

$$Z_v^* = (4Z_i^5 - 4Z_fZ_i^4 + Z_f^2Z_i^3)^{1/5} \quad (20)$$

and thus enforces asymptotic agreement between length and velocity representations for a given value of Z_i .

3. Results

3.1. Low-energy photoionization cross section

In table 1 the calculated *ab initio* PCS values are listed for the length and velocity forms of the dipole operator. Remarkable agreement of the order of 10^{-3} Mb can be noticed between these two formulations that for exact wavefunctions yield identical results. The results are given for the optimal values

Table 1. Total photoionization cross sections σ (in Mb) for He as a function of the photon energy E (in eV). The present results are compared with the experimental values of Samson *et al* [1] and with the B -spline calculations of Venuti *et al* [6].

E	This work		Venuti <i>et al</i> [6]		σ_{exp}
	σ_l	σ_v	σ_l	σ_v	
24.596	7.385 44	7.383 69	7.397 14	7.396 76	7.40
25	7.208 85	7.209 65	7.220 37	7.220 10	7.21
26	6.795 41	6.795 24	6.799 59	6.799 46	6.79
27	6.407 43	6.407 05	6.411 03	6.410 87	6.40
28	6.043 41	6.042 24	6.044 42	6.044 12	6.05
29	5.703 23	5.702 31	5.705 46	5.704 99	5.70
30	5.385 96	5.385 55	5.388 66	5.388 02	5.38
31	5.090 35	5.089 60	5.092 60	5.091 85	5.10
32	4.814 60	4.814 01	4.816 68	4.815 86	4.82
33	4.557 79	4.557 18	4.559 60	4.558 78	4.57
34	4.318 50	4.317 51	4.319 96	4.319 18	4.32
35	4.095 19	4.095 60	4.096 42	4.095 71	4.09
36	3.886 78	3.887 22	3.887 71	3.887 07	3.88
37	3.692 17	3.691 42	3.692 77	3.692 20	3.68
38	3.510 38	3.509 66	3.510 75	3.510 24	3.50
39	3.340 37	3.339 81	3.340 78	3.340 32	3.32
40	3.181 27	3.180 72	3.181 73	3.181 29	3.16
41	3.032 27	3.031 68	3.032 60	3.032 17	3.01
42	2.892 63	2.893 35	2.802 95	2.892 51	2.86
43	2.761 74	2.762 47	2.762 17	2.761 71	2.72
44	2.638 92	2.639 66	2.639 31	2.638 82	2.60
45	2.523 60	2.524 37	2.523 95	2.523 44	2.48
46	2.415 26	2.416 07	2.415 72	2.415 19	2.38
47	2.313 41	2.313 62	2.313 87	2.313 32	2.28
48	2.217 81	2.217 78	2.218 20	2.217 64	2.19
49	2.127 92	2.127 90	2.128 30	2.127 73	2.10
50	2.043 44	2.043 46	2.043 73	2.043 17	2.02
51	1.964 12	1.964 16	1.964 42	1.963 88	1.94
52	1.889 76	1.889 86	1.889 99	1.880 46	1.85
53	1.820 26	1.820 46	1.820 49	1.819 99	1.77
54	1.755 62	1.755 96	1.755 84	1.755 37	1.71
55	1.696 24	1.696 92	1.696 39	1.695 94	1.67
56	1.642 83	1.643 47	1.642 89	1.642 47	1.63
57	1.597 40	1.597 97	1.597 34	1.596 95	1.61
58	1.566 12	1.566 68	1.566 06	1.565 69	1.58
59	1.577 22	1.577 41	1.576 56	1.576 18	1.56

θ_{opt} obtained according to equation (4). However, overall, only a very small variation of the PCS with θ is found which indicates that the used basis set is rather complete for the considered energy range.

Table 1 also compares the present results with the experimental data of Samson *et al* [1] and the supposedly most accurate previous calculation of Venuti *et al* [6]. If shown graphically, as in figure 1, there are almost no visible differences between the various theoretical and experimental results.

The very good agreement of the present results with the ones in [6] is confirmed in figure 2 that shows the relative deviation to the present length-form data for photon energies below 59 eV. Despite the completely different theoretical approaches the agreement is remarkably good, since the deviation is less than 0.17% and especially in the energy range from 38 to 58 eV the relative deviation is of the order of $\pm 0.03\%$ (except for the values in [6] at 42 eV (length form) and at 52 eV (velocity form), which we suggest to

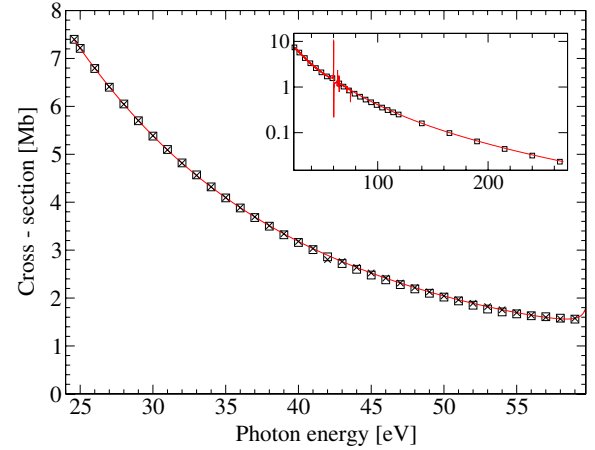


Figure 1. Total photoionization cross section of helium ($1S$ ground state) from the ionization threshold to 59 eV (red line: this work, cross: theoretical values of Venuti *et al* [6], open square: experimental values of Samson *et al* [1, 2]). The inset shows the theoretical PCS of this work and the experimental values of Samson *et al* on a logarithmic scale also extending to larger photon energies.

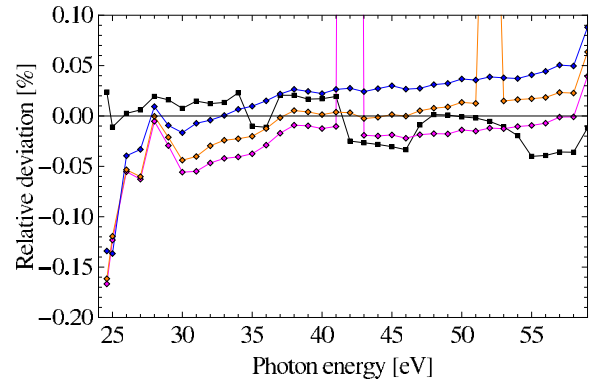


Figure 2. Relative deviation of our results in velocity form (black square) and of the results of Venuti *et al* [6] (diamond) in length (orange), velocity (magenta) and acceleration forms (blue) from the helium photoionization cross section calculated in this work within the length formulation.

be typos). Figure 2 also shows the deviation between our results in length and velocity forms. Again good agreement with deviations less than $\pm 0.04\%$ is found. In an earlier work, Chang and Fang adopted [22] a theoretical approach that is practically identical to the one used in [6], but a smaller basis set was used. Our results also agree well with the ones in [22] (relative error of about 0.1%), but are consistently in better agreement with the ones in [6]. Clearly, on this level of accuracy convergence of the adopted basis set is finally decisive, while the two completely different approaches (B splines with box discretization versus STOs with complex scaling) appear to yield identical results within the achieved level of convergence. This indicates the correct and numerically stable implementation of both approaches. In fact, in the case of the single data point (at 40 eV) given within the energy range shown in figure 2, the result of the Floquet calculation by Ivanov and Kheifets [8] also agrees within 0.03% with our results and the one in [6]. Therefore, three

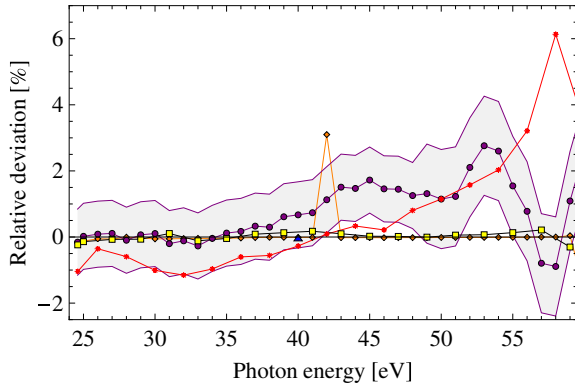


Figure 3. Relative deviation from the helium photoionization cross section calculated in this work (length form): theoretical data of Venuti *et al* [6] (orange diamond, length form), Chang and Fang [22] (yellow square, length form), as well as Ivanov and Kheifets (single point at 40 eV, blue triangle) [8], the experimental values of Samson *et al* [1, 2] (violet circle) and the compiled data of Yan *et al* [23] (red asterisk). The shaded area illustrates the error range estimated by Samson *et al* for their experiment ($\pm 1\%$ until 48 eV and $\pm 1.5\%$ starting from 49 eV).

different theoretical approaches agree within an extremely small relative error.

On the other hand, the experimental helium PCS of Samson *et al* [1, 2] is still the primary reference for benchmarks and comparison, despite the fact that recent numerical calculations [6, 8] yielded cross sections that differ from the experimental values outside the estimated experimental error bars. In view of the already discussed very good agreement with the theoretical data in [6] (figure 2), we confirm the deviations to the experimental data in [1, 2] outside the error bars. This can be clearly seen in figure 3. For photon energies between 51 and 55 eV the relative deviation of the results of Samson *et al* from our data and also from the ones of Venuti *et al* is evidently above the error of $\pm 1.5\%$ estimated by Samson *et al* [1, 2]. The largest deviation of approximately 2.6% in comparison to our values occurs at 53 and 54 eV. These deviations appear to be too large to be explained by a failure of the approximations adopted in the present calculation. Neither effects due to the finite size of the nucleus nor relativistic effects should be of a magnitude that is sufficient for explaining such a discrepancy that in addition would have to be strongly photon-energy dependent. As is discussed below, on the basis of the derived analytical high-energy tail, also the consideration of non-dipole terms and thus a breakdown of the dipole approximation yields corrections that are orders of magnitudes smaller than the ones required to find agreement between theory and experiment.

In view of the importance of the He PCS discussed in the introduction, data sets also exist that represent a compilation of experimental and theoretical data and try to cover large photon-energy ranges. Such a data set was reported by Yan *et al* [23] and was claimed by its authors to be reliable for all energies. The comparison in figure 3 shows that agreement with the here considered theoretical results is reasonable, but not really good. In fact, at both ends of the shown energy range the agreement of the theoretical data

with the compiled ones is less good than the one found for the experimental data in [1, 2]. Since the compiled data lie below the theoretical ones for low energies and above for larger energies, the agreement is only good for intermediate energies close to the crossing point at about 42 eV. Especially close to the ionization threshold the experimental data in [1, 2] appear to be clearly superior to the compiled ones in [23]. In fact, within the first 10 eV above the ionization threshold the experimental data are in remarkable agreement to theory with a deviation of less than about 0.15%.

3.2. High-energy photoionization cross section

Motivated by the recent work of Ivanov and Kheifets [8] who claim an even larger deviation from the experimental data of Samson *et al* for larger photon energies than for the lower ones considered in [6], we also studied the single-photon ionization process in the non-resonant energy regime above the He⁺ ionization threshold ($E \approx 79$ eV).

Although our approach, the expansion of the two-electron wavefunction in STOs, was originally developed for bound-state transitions, the extension by the complex-scaling method also provides an excellent description of high-energy continuum states of the He atom [9]. Figure 4 shows the deviation of various theoretical, experimental and compiled data from our results for energies between 80 and 205 eV. The agreement with an older *B*-spline calculation by Decleva *et al* [7] is by far not as good as the one found with the later work [6] of the same authors that concentrated on the low-energy regime. However, the deviation of our values from the Floquet results of Ivanov and Kheifets [8] is for most of the data points less or equal to about 0.03%. Only at the highest energy, 205 eV, a deviation of 0.37% is found. Therefore, we again confirm the discrepancy between previous theoretical calculations and the experimental reference data of Samson *et al*, this time reaching to about 6% at 80 eV, as can also be seen from the comparison of the different results in table 2.

On the other hand, we find in the energy range between about 110 and 160 eV a deviation from experiment that remains basically below 2%. Furthermore, the compiled data of Yan *et al* [23] agree in this complete energy interval better with the theoretical results than the experimental results of Samson *et al*, in contrast to the findings at lower photon energies. In the energy interval between about 80 and 100 eV the experimental values reported by Bizau and Wuilleumier [24] deviate from our calculation in a qualitatively very similar fashion as the experimental data of Samson *et al*. However, quantitatively, the deviation is smaller and remains in between 3 and 5%. On the other hand, in between 100 and 150 eV the data in [24] are substantially smaller than our theoretical results, leading to a deviation of up to 7%. For the higher energies shown in figure 4 the deviation of both experimental data sets from our results is again qualitatively similar, but the ones of Bizau and Wuilleumier lie below our results and approach the latter with increasing energy, while the ones of Samson *et al* lie above and thus agreement with our data becomes worse for increasing photon energy.

Table 2. Total photoionization cross sections σ for He at high photon energies E (in eV). Until $E = 250$ eV the σ values are given in Mb and our results stem from the full *ab initio* calculation. Starting from 400 eV the results for the model tail (11) and (12) are given ($Z_i = 1.5293$, $Z_v = 1.7455$; $Z_f = 1$) and all σ values are in Barn. Our results are compared to the experimental values of Samson *et al* [1], the *B*-spline calculation of Decleva *et al* [7] and the Floquet results of Ivanov and Kheifets [8].

E	This work		Decleva <i>et al</i> [7]		Samson <i>et al</i> [1]	Ivanov <i>et al</i> [8]
	σ_l	σ_v	σ_l	σ_v	σ_{exp}	σ_{FI}
80	0.737 21	0.737 77	0.759	0.74	0.693	0.7369
85	0.630 41	0.630 99	—	—	0.595	0.6308
91	0.527 08	0.527 62	—	—	0.502	0.5272
95	0.470 11	0.470 63	—	—	0.45	0.4701
100	0.409 60	0.410 04	0.417	0.403	0.393	—
111	0.308 08	0.308 54	—	—	0.3	0.3082
120	0.248 09	0.248 63	0.251	0.243	0.244	—
140	0.160 41	0.161 08	0.167	0.158	0.160	—
160	0.109 24	0.109 85	0.112	0.108	0.108	—
180	0.077 49	0.077 99	0.802	0.077	0.076	—
205	0.052 70	0.053 21	—	—	0.051	0.0529
250	0.028 81	0.029 39	0.0306	0.0293	0.0277	—
400	6561	6812	7270	7009	6370	—
600	1785	1871	2001	1940	1770	—
1000	335	354	395	384	339	—
2000	33.1	35.2	39.5	40	34.8	—
3000	8.42	8.96	—	—	8.77	—
4000	3.17	3.38	—	—	3.20	—
5000	1.48	1.58	—	—	1.47	—
6000	0.79	0.85	—	—	0.77	—
7000	0.47	0.50	—	—	0.45	—
8000	0.30	0.32	—	—	0.28	—

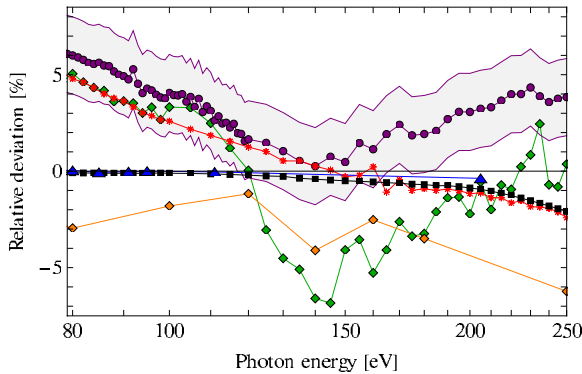


Figure 4. Relative deviation from the helium photoionization cross section calculated in this work (length form): present *ab initio* calculation in velocity form (black square), Floquet calculation of Ivanov and Kheifets [8] (blue triangle), *B*-spline calculation of Decleva *et al* [7] (orange diamond), experimental data measured by Samson *et al* [1] (violet circle) or Bizau and Wuilleumier [24] (green diamond) and the compiled values by Yan *et al* [23] (red asterisk). The shaded area illustrates the error range estimated by Samson *et al* for their experiment ($\pm 2\%$).

For very high photon energies above 300 eV we propose to use the analytical model tails introduced in equations (11) and (12). Within the model, two of the three parameters, Z_f and I , are fixed by the sum of the charges of the remaining particles and the either experimentally or theoretically known ionization potential, respectively. On the other hand, the choice of the parameter Z_i (Z_v) for the tail in length (velocity) representation is less evident. One possibility is to relate it to the ionization potential *via* $Z_i = \sqrt{2I}$ which leads to a completely parameter-free model tail [15, 16]. A second way

to obtain a parameter-free tail is based on the requirement to yield the best possible ground-state description when adopting the trial wavefunction of (10) in a variational calculation. For He this results in the mean-field value $Z_i = 1.6875$ [17] compared to about 1.34 for $Z_i = \sqrt{2I}$. In a third alternative Z_i is kept as a free parameter. In this case it is chosen in such a way that it provides the best agreement of the resulting tail with some *ab initio* or experimental PCS, within some finite energy interval. The motivation for fitting Z_i is the fact that an independent-particle description is a rather crude approximation especially for the correlated initial two-electron state. The fit may thus at least partly compensate this deficiency.

When performing a least-squares fit of the tail to our *ab initio* calculation in the energy range from 136 to 272 eV we obtain $Z_i = 1.5293$. This value lies in between the prediction based on either $Z_i = \sqrt{2I} = 1.34$ or the mean-field result, $Z_i = 1.6875$. Note, although the chosen fit interval spans only a very small energy region of the PCS, the extrapolated PCS agrees, in a much larger energy range, well with the *ab initio* results. In the shown energy range from 300 eV to 8 keV that lies completely outside the fit interval and is more than 50 times larger very good agreement is found with the experimental data of Samson *et al* (figure 5). In fact, we found almost the same effective initial charge, $Z_i = 1.53 \pm 0.01$, when alternatively fitting the tail to the experimental data of Samson *et al*. The indicated uncertainty in Z_i arises from different starting points of the energy interval used in the fit procedure, while the end point was always chosen at an energy of 8 keV.

In figure 6 the already discussed tail with fitted Z_i is compared to the case that Z_i is fixed to its mean-field value

Table 3. Parameters for the model tail for various one- and two-electron systems.

Parameters	H ⁻	H	He	He ⁺	Li ⁺	HeH ⁺
Z_i	0.5586	1	1.5293	2	2.5191	1.9414
Z_v	0.7662	1	1.7455	2	2.7390	1.9026
Z_v^*	0.7371	1	1.7224	2	2.7152	1.9177
Z_v^-	0.6875	1	1.6875	2	2.6875	1.8186 ^a
Z_f	0	1	1	2	2	2
N	2	1	2	1	2	2
I (eV)	0.754 36	13.606	24.5912	54.4234	75.64	45

^a For HeH⁺ the mean-field value was estimated from the ionization potential as $Z_v^- = \sqrt{2I}$.

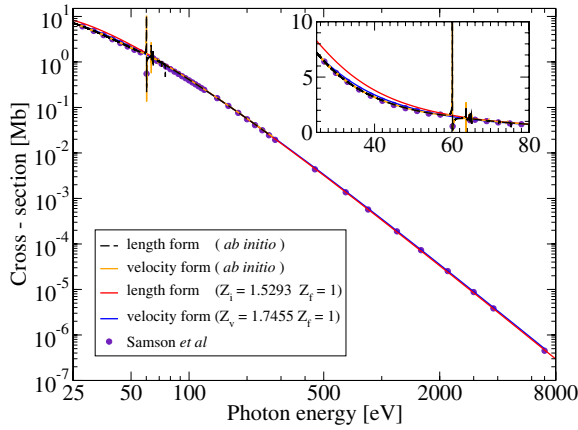


Figure 5. The analytical model tails for different representations of the dipole operator (length form: red line, velocity form: blue line) using the respective optimal parameters Z_i and Z_v are compared to the present *ab initio* results (length form: black line, velocity form: orange line) and the experimental data of Samson *et al* (violet circle). The inset shows the same curves for low energies on a linear scale. (Due to the good agreement, most curves are almost indistinguishable.)

(1.6875) while Z_f is used as a fit parameter. The resulting tail lies in this case above the experimental data of Samson *et al*. While the slope differs for photon energies at about 300 eV, an almost constant off-set is found between the tail and the experimental data for large energies, if plotted on a doubly logarithmic scale. A further off-set is observed, if all tail parameters are fixed on the basis of simple arguments, i.e. the initial charge Z_i is set to the mean-field value 1.6875 and the final charge Z_f to the value 1.0 that should be appropriate at very large separation of the ejected electron. Not shown is the tail that is obtained under the assumption of no relaxation ($Z_i = Z_f$), since this tail does not agree to the experimental data at all.

A similar analysis can be performed for the velocity-form representation of the model tail. By applying the same fit procedure for obtaining $\tilde{\sigma}_0^V$ as was used for the length form we find $Z_v = 1.7455$. It may be observed that this result is close to the mean-field value 1.6875. This may indicate that, if one would like to avoid the fit or if no data are available for performing a fit, the best choice for a parameter-free tail is the tail in velocity form adopting the mean-field prediction for Z_v (figure 6).

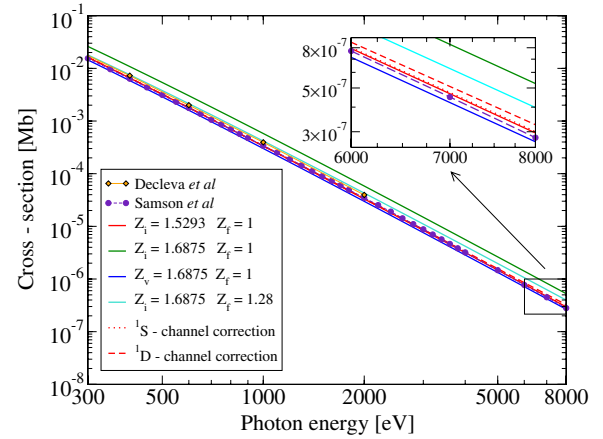


Figure 6. The analytic tails (see equations (11) and (12), solid lines) that are an approximation to the photoionization cross section of He at high energies are shown for different parameters Z_i , Z_f (length-form tail) and Z_v , Z_f (velocity form) and compared to the experimental values of Samson *et al* [1] (violet circle) and the calculation of Declewa *et al* [7] (orange diamond). The dotted and dashed lines show the first-order corrections to the dipole approximation according to equation (14) due to final states with S or D symmetry, respectively. The inset shows the high-energy part of the spectrum on a linear scale.

Using equation (20) and the length-form result $Z_i = 1.5293$ we can derive $Z_v^* = 1.7224$. Clearly, the independently obtained values for Z_v and Z_v^* are in quite reasonable agreement. Thus we conclude that the model tail, although it is derived with approximate wavefunctions, yields for very high energies the required independence of the chosen representation (length or velocity form) of the dipole operator. Furthermore, because the results of equation (20) and the fit are in very good agreement, it is evident that the fit procedure is most suitable to derive the parameter values for the model tail. Finally, we derived the asymptotic limit of the PCS of helium to $\tilde{\sigma}_0^{\text{He}}(E) \approx 487.945 E (\text{keV})^{-7/2}$. The pre-factor is consistent with the values discussed by Samson *et al* for different experimental data.

In figure 5 the length and velocity model tails are plotted for their optimal values. It can be observed that the photon energy where the model tail approaches the *ab initio* calculation is lower for the velocity form than for the length form. In fact, it is quite surprising how well the velocity-form tail agrees to the full *ab initio* results and the experimental data even down to the ionization threshold. This superiority

of the velocity form compared to the length form found at low energies is, however, on the first glance a little bit surprising, since the transition dipole matrix elements in length form are usually supposed to be preferable at low photon energies [8, 25]. This is often explained by the lower sensitivity of the length-form matrix elements to errors in the long-range part of the wavefunctions and the fact that low-energy transitions are more sensitive to this long-range part. However, it may be remembered that the obtained value of Z_v is quite close to the mean-field prediction Z_v^- . Since the low-energy part of the photoionization spectrum is more sensitive to the details of the atomic potential, a model like the velocity-form tail, that is closer to the mean-field prediction, may thus be favourable compared to the length-form tail with a rather different value found for the corresponding parameter Z_i .

In order to demonstrate the generality of the analytical tail, we investigated its applicability to other two-electron systems. Besides the neutral helium atom we considered the hydrogen anion, the lithium cation, and even the HeH^+ molecular cation. The used tail parameters are listed in table 3. Figure 7 shows a comparison of the tails for these systems with the corresponding literature data and, for the atoms, also with *ab initio* results calculated in this work. The found agreement is in all cases good or even very good. This indicates the universality of the tail concept. It is, in fact, interesting that the tail works well even for a system like H^- in which the escaping electron experiences within the tail model no influence from the remaining hydrogen atom, since polarization effects are ignored. Furthermore, the initial state of H^- is only bound due to correlation and thus a mean-field model is in principle not applicable. Nevertheless, also in this case the tail seems to work quite well. In the case of HeH^+ a high-energy tail had been proposed before [12], but a parameter-free tail (with $Z_i = Z_f = \sqrt{2I}$) had been used. The result is also shown in figure 7. It also compares reasonably well with the full *ab initio* results. The reason is that in this case Z_i is very close to Z_f and even also to $\sqrt{2I}$. In fact, in this work the mean-field value of Z_v^- for HeH^+ has also been estimated from $\sqrt{2I}$, since a one-centre mean-field calculation restricted to s-type orbitals turns out to be ambiguous, because the result depends on the choice of the orbital position. Note, for a molecular system there is the additional complication due to nuclear motion. However, in the spirit of the high-energy tail it should have a negligible influence on the high-energy part of the photoionization spectrum. Therefore, the tail is formally obtained for a single internuclear separation, usually the equilibrium distance. Here, we chose in agreement to [12] the ionization energy $I = 45$ eV.

According to (14) the model tail provides the possibility of giving an analytical estimate of the first-order correction to the dipole approximation. The two contributions from final states with S and D symmetry are also shown in figure 6. While the D contribution is clearly dominant, the total correction to the dipole approximation is still negligibly small at photon energies of several keV. Note, however, that the relative contribution reaches already 11% at 8 keV due to the very small cross section of less than 1 barn. This allows us to conclude that very accurate studies of the PCS of He performed

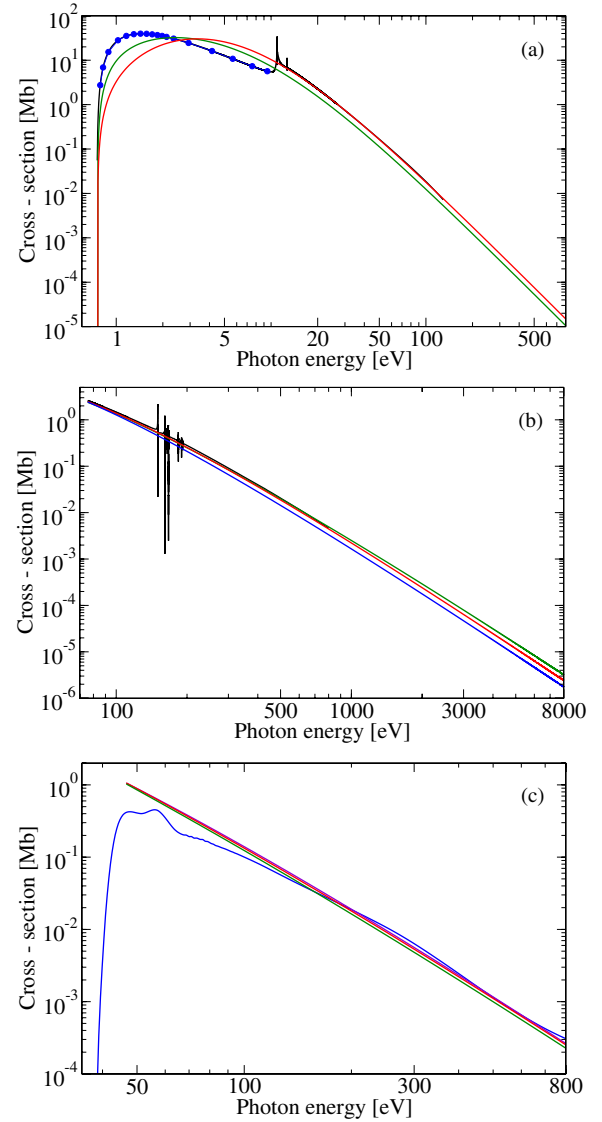


Figure 7. Analytical model tails (length form with optimal values for Z_i , red solid lines) for different two-electron systems are compared to literature data. (a) H^- : Venuti and Decleva [26] (blue circle), (b) Li^+ : Verner *et al* [27] (blue line) and (c) HeH^+ (parallel contribution): Saenz [12] (blue line). Also shown (green lines) are the results for the tail in velocity form using the mean-field value Z_v^- . For the atoms (a) and (b) *ab initio* cross sections obtained within this work are also shown (black solid lines), while for HeH^+ the alternative tail proposed in [12] is additionally given (purple solid line).

in the keV photon energy range must take corrections to the dipole approximation into account. However, since the correction is proportional to the squared photon energy and the cross section itself increases by almost five orders of magnitude when going from 8 keV to 300 eV photons, corrections due to a breakdown of the dipole approximation are negligible within the here considered level of accuracy for photon energies below 200 eV. Therefore, the deviations between the theoretical results of this work and the ones in [26] or [8] from the experimental reference data of Samson *et al* [1, 2] or Bizau and Wuilleumier [24] cannot be explained by a failure of the dipole approximation.

4. Summary

A non-relativistic *ab initio* calculation of the photoionization cross section of He has been performed for photon energies covering the non-resonant part of the spectrum from the ionization threshold until about 250 eV. An analytical high-energy model tail has been introduced and the *ab initio* data were used in order to determine the single fit parameter. With this tail it became possible to extend the photoionization spectrum to arbitrarily large photon energies within the underlying non-relativistic dipole approximation. Furthermore, the first-order correction to the dipole approximation could be estimated analytically with the aid of the model tail.

Our theoretical results agree extremely well with the ones obtained by different theoretical approaches in the low- and the high-energy parts by Venuti *et al* [6] and Ivanov and Kheifets [8], respectively. Therefore, we confirm the pronounced deviation between theoretical and experimental results noted in those earlier works. Particularly, at the photon-energy range around 50 eV that is very relevant to present-day FELs like FLASH or high-harmonic sources the relative deviation is unambiguously larger than the error estimates of the experiment of Samson *et al* [1, 2]. We want to stress that all theoretical data sets compared in this work are based on different approaches where each of them has its own advantages and disadvantages. The goal is not to prove the present approach to be superior, but to confirm the deviations between theory and experiment using a completely different theoretical approach. It is clear that the observed extremely good agreement shows the high level of convergence of the various theoretical results and reveals that important effects like, e.g., the electron–electron correlation of the ground state were considered properly in all of them.

As we also demonstrated the validity of the dipole approximation at least for photon energies up to 200 eV where the previous comparisons were performed, this possible source of disagreement between theory and experiment is excluded. Since relativistic effects especially close to the ionization threshold are expected to be smaller than the found deviations between theory and experiment we conclude that the quality of theoretical calculations of the helium photoionization cross section appears to have reached a consistently higher level than the experiment. In view of the fundamental importance of the photoionization cross section of helium we hope that this work stimulates future efforts to resolve the discrepancies between theory and experiment. On the theory side, an explicit consideration of relativistic effects would be required to finally remove possible doubts that they are responsible for the found discrepancy between the non-relativistic calculations and experiment. It should be stressed that such relativistic corrections are required to have a rather pronounced photon-energy dependence even in the non-resonant regime, if they should be able to explain the deviations between theory and

experiment. This appears to make such an explanation even less likely. Until further experimental or theoretical progress has been achieved, we propose to use the theoretical *ab initio* results, especially the ones of this work that cover a large photon energy range up to about 250 eV in a consistent fashion, instead of the experimental ones as reference data for, e.g., calibrating new light sources, since they appear to be more accurate and reliable. For higher energies the proposed hydrogenic tail based on a fit to our *ab initio* data in between 136 and 272 eV was shown to provide a reliable estimate, or at least a good interpolation between the sparse experimental data points.

Acknowledgments

The authors acknowledge financial support from the *COST programme CM0702* and the *Fonds der Chemischen Industrie*. This work was supported in parts by the National Science Foundation under grant no NSF PHY05-51164.

References

- [1] Samson J A R, He Z X, Yin L and Haddad G N 1994 *J. Phys. B: At. Mol. Opt. Phys.* **27** 887
- [2] Samson J A R and Stolte W C 2002 *J. Electron Spectrosc. Relat. Phenom.* **123** 265
- [3] Wellhöfer M, Hoeft J T, Martins M, Wurth W, Braune M, Viehhaus J, Tiedtke K and Richter M 2008 *J. Instrum.* **3** P02003
- [4] Nagasono M *et al* 2007 *Phys. Rev. A* **75** 051406
- [5] Mitzner R *et al* 2009 *Phys. Rev. A* **80** 025402
- [6] Venuti M, Decleva P and Lisini A 1996 *J. Phys. B: At. Mol. Opt. Phys.* **29** 5315
- [7] Decleva P, Lisini A and Venuti M 1994 *J. Phys. B: At. Mol. Opt. Phys.* **27** 4867
- [8] Ivanov I A and Kheifets A S 2006 *Eur. Phys. J. D* **38** 471
- [9] Stark A and Saenz A 2010 *Phys. Rev. A* **81** 032501
- [10] Fano U and Cooper J W 1968 *Rev. Mod. Phys.* **40** 441
- [11] Rescigno T N and McKoy V 1975 *Phys. Rev. A* **12** 522
- [12] Saenz A 2003 *Phys. Rev. A* **67** 033409
- [13] Saenz A, Weyrich W and Froelich P 1993 *Int. J. Quantum Chem.* **46** 365
- [14] Jian-Jie W and Chen-Zhong D 2009 *Chin. Phys. B* **18** 3819
- [15] Barbieri R S and Bonham R A 1991 *Phys. Rev. A* **44** 7361
- [16] Saenz A and Froelich P 1997 *Phys. Rev. C* **56** 2162
- [17] Bethe H A and Salpeter E E 1977 *Quantum Mechanics of One- and Two-Electron Atoms* (New York: Plenum)
- [18] Saenz A 2000 *J. Phys. B: At. Mol. Opt. Phys.* **33** 4365
- [19] Saenz A 2000 *Phys. Rev. A* **61** 051402
- [20] Lühr A, Vanne Y V and Saenz A 2008 *Phys. Rev. A* **78** 042510
- [21] Wang S 1999 *Phys. Rev. A* **60** 262
- [22] Chang T N and Fang T K 1995 *Phys. Rev. A* **52** 2638
- [23] Yan M, Sadeghpour H R and Dalgarno A 1998 *Astrophys. J.* **496** 1044
- [24] Bizau J M and Wuilleumier F J 1995 *J. Electron Spectrosc. Relat. Phenom.* **71** 205
- [25] Johnston R R 1964 *Phys. Rev.* **136** A958
- [26] Venuti M and Decleva P 1997 *J. Phys. B: At. Mol. Opt. Phys.* **30** 4839
- [27] Verner D A, Ferland G J, Korista K T and Yakovlev D G 1996 *Astrophys. J.* **465** 487